Jurnal Polimesin
Department of Mechanical Engineering
State Polytechnic of Lhokseumawe
http://e-jurnal.pnl.ac.id/polimesin

e-ISSN : 2549-1999 No. : 1 Month : February
p-ISSN : 1693-5462 Volume : 24 Year : 2026

Processing dates: received on 2025-10-17, reviewed on 2025-12-18, accepted on 2025-12-31 and online availability on 2026-02-28

The impact of nozzle temperature on the shrinkage of annealed 3D printed PLA

Sugianto[1], Meriatun[1], Pristiansyah[1], Ramli[1], Atikah Araminta Wardiyah[1], Hasdiansah[1]*, Herianto[2]
[1]Department of Mechanical Engineering, Bangka Belitung State Manufacturing Polytechnic, Sungailiat 33211, Indonesia
[2]Department of Mechanical and Industrial Engineering, Gadjah Mada University, Yogyakarta, 55281, Indonesia
*Corresponding author: phiannttarah@yahoo.co.id

Abstract

Thermal annealing is used to strengthen the mechanical performance and thermal stability of fused deposition modeling (FDM) parts made from polylactic acid (PLA). This treatment frequently introduces dimensional shrinkage, compromising geometric accuracy and limiting the reliability of printed components in demanding applications. Among the printing parameters, nozzle temperature is a key variable because it influences melting behavior, interlayer diffusion, and the buildup of internal stresses, yet its role in managing shrinkage after annealing has not been clearly established. This study evaluates the influence of nozzle temperature on the anisotropic shrinkage of annealed PLA specimens across different specimen lengths and measurement directions (X and Y), with the main analysis conducted at selected nozzle temperatures ranged 195-230°C. Dimensional changes were quantified before and after annealing at 100°C for 60 min, and statistical evaluation was performed using analysis of variance (ANOVA) with post-hoc testing based on replicated specimens. The results confirm nozzle temperature as a significant contributor to shrinkage behavior, $F(2,36) = 30.90$, $p < 0.001$, partial $\eta^2=0.63$. Printing at 230°C consistently yielded the smallest dimensional reduction, outperforming both 210°C and 220°C. Within the examined range, 230°C emerges as the most effective nozzle setting for minimizing annealing-induced shrinkage, offering a practical processing window to improve dimensional accuracy and functional reliability in FDM-printed PLA parts.

Keywords:
Fused deposition modeling, polylactic acid, annealing, shrinkage, nozzle temperature.

1 Introduction

Fused Deposition Modelling (FDM) is one of the most widely used additive manufacturing techniques, in which three-dimensional objects are fabricated by the layer-by-layer extrusion of thermoplastic filaments [1]. Due to its cost-effectiveness, precision in prototyping, and accessibility to users, FDM has gained extensive adoption across multiple industrial sectors, including biomedical devices [2], aerospace [3], and automotive components [4], [5]. Despite these advantages, the technology continues to face notable limitations, including high material consumption costs, relatively slow production rates, and restrictions on part dimensions [6]. In addition, critical process parameters, particularly nozzle temperature, strongly influence part quality, governing warpage, dimensional stability, and overall accuracy [7], [8]. Appropriate nozzle temperature promotes effective interlayer adhesion, thereby improving structural integrity and reducing the likelihood of deformation [9].

PLA, a biodegradable aliphatic polyester, has become one of the most prominent materials for FDM printing [10]. Its appeal arises from its renewable feedstocks, relatively low melting temperature, ease of processing, biodegradability, and balanced mechanical performance [11], [12]. For these reasons, PLA has become the preferred filament material for both prototyping and functional parts. Nevertheless, its performance can be further optimized through process control-such as adjusting bed temperature, nozzle speed, or raster orientation-and through post-processing strategies, such as annealing, to enhance impact resistance and thermal stability [13]. Additionally, PLA's mechanical strength can be improved by reinforcement with fillers, thereby forming PLA-based composites with superior performance [14].

Among post-processing strategies, annealing is widely employed to increase crystallinity and relieve residual stresses generated during printing [15], [16]. By heating the polymer above its glass transition temperature (Tg), annealing enables molecular rearrangement, which enhances tensile strength and thermal resistance [17]. However, annealing often introduces undesirable dimensional variations, particularly anisotropic shrinkage: contraction along the x- and y-directions and expansion along the z-direction [18]. Such distortions present a major barrier to achieving the dimensional accuracy required for functional applications.

Previous studies suggest that nozzle temperatures in the range of 220-240°C are essential to achieving high-quality PLA parts with improved mechanical performance [19]. In addition, studies employing nozzle temperatures between 180 and 230°C have emphasized the role of thermal history during deposition in promoting polymer melt diffusion and interlayer re-entanglement, thereby enchancing interlayer adhesion and mechanical performance [20]. Despite these insights, there remains a lack of systematic investigations directly linking nozzle temperature variation to the degree of shrinkage observed after annealing. This knowledge gap is significant, particularly in the context of growing reliance on FDM for functional prototypes and end-use components that demand strict dimensional precision [21]. In addition to nozzle temperature, geometric factors such as specimen length and measurement direction can influence thermal history, residual stress distribution, and anisotropic dimensional changes in FDM-printed parts; therefore, these factors are considered in the present study to ensure consistency with the multifactorial statistical analysis.

Accordingly, the primary research question of this study is whether variations in nozzle temperature significantly influence the magnitude and anisotropy of dimensional shrinkage in PLA parts subjected to thermal annealing. This study addresses the gap by systematically evaluating the influence of nozzle temperature on the anisotropic dimensional shrinkage of annealed PLA specimens. The outcomes are expected to provide guidance for identifying optimal printing parameters that minimize shrinkage, maintain geometric accuracy, and enhance the overall quality and reliability of FDM-fabricated PLA components.

2 Research methodology

The methodology consisted of four main stages: selection of materials, fabrication of test specimens, surface preparation and dimensional measurement, and statistical data analysis.

2.1 Material

Commercial-grade PLA filament with a 1.75 mm diameter was selected as the feedstock material. All specimens were fabricated using an FDM 3D printer equipped with a 0.4 mm nozzle. To maintain structural uniformity, the following fixed parameters were applied: a printing speed of 50 mm/s, a layer height of 0.3 mm, and a concentric infill pattern.

2.2 Fabrication of samples

An exploratory set of specimens was initially fabricated at nozzle temperatures of 195, 200, and 205°C to observe the general

shrinkage response and to guide the selection of temperatures for the subsequent targeted experiment. This preliminary step provided insight into whether shrinkage exhibited a positive or negative relationship with nozzle temperature. Based on these findings, a refined set of target temperatures was chosen for detailed experimentation. The subsequent targeted experiment was conducted at nozzle temperatures of 210, 220, and 230°C, with three replicated specimens (n=3) produced at each temperature. This approach ensured both broad trend identification and rigorous statistical evaluation. The planned specimens to be used can be seen in Table 1.

Table 1. Specimen preparation

Nozzle- Temp.	X x Y x Z (mm)	Repetition	Measurement axes	Annealed (min)
Intial temp.	20 × 15 x 10	3	x and y	30
Target Temp.	20 × 30 x 30	3	x and y	60
	20 × 20 x 20	3	x and y	60
	20 × 10 x 10	3	x and y	60

2.3 Surface preparation and initial measurement

After printing, the specimen surfaces were carefully smoothed with fine-grit sandpaper to eliminate irregularities and enhance measurement precision. Dimensional measurements were obtained using a digital caliper (±0.01 mm accuracy). For each measurement direction (X and Y), three readings were recorded: two at the specimen ends and one at the midpoint. The same procedure was repeated after annealing. Dimensional shrinkage was calculated as the percentage difference between the pre- and post-annealing measurements.

2.4 Statistical analysis

For the preliminary screening, shrinkage data were evaluated to identify general trends. Because only one specimen was produced at each temperature and the X and Y measurements were identical, a two-way analysis of variance was applied. In contrast, the targeted experiment employed replicated specimens with distinct X and Y shrinkage values, and a three-way ANOVA was conducted to assess the main effects of nozzle temperature, specimen length, and measurement direction (X and Y), as well as their interactions, on dimensional shrinkage.

Prior to analysis, the assumptions of normality and homogeneity of variance were tested. Normality of residuals was evaluated using the Shapiro-Wilk test and verified through inspection of quantile–quantile (Q-Q) plots. Homogeneity of variances was examined using Levene's test. In cases where normality was not satisfied, percentage shrinkage data were subjected to an arcsine square-root transformation, a well-established method for stabilizing variance in proportional datasets [22]. This transformation is recognized as robust for meeting the assumptions required in factorial ANOVA designs [23]. When significant interaction effects were identified, post-hoc pairwise comparisons were performed using Tukey's Honest Significant Difference (HSD) test to distinguish differences between specific group means. A significance threshold of α=0.05 was applied for all statistical evaluations.

3 Result and discussion

3.1 Initial temperature

The dimensional measurements of specimens printed at nozzle temperatures between 195 and 205°C, obtained before and after annealing at 100°C for 30 minutes, are summarized in Tables 2 and 3. The corresponding distributions of the data were further examined through quantile–quantile (Q-Q) plots, as illustrated in Fig.1, to visually assess normality.

Table 2. Shrinkage in X-direction

Temp.	Length	Shrinkage (%)	Sorted R.	Percentile	Normal Q	Sample Q
195 °C	20	2.98	-0.41	0.0556	-1.5932	-1.7861
		2.34	-0.26	0.1667	-0.9674	-1.1473
		2.92	-0.15	0.2778	-0.5895	-0.6485
200 °C	20	2.81	0.01	0.3889	-0.2822	0.0523
		2.60	0.03	0.5000	0.0000	0.1130
		2.32	0.14	0.6111	0.2822	0.5962
205 °C	20	1.43	0.17	0.7222	0.5895	0.7574
		1.55	0.23	0.8333	0.9674	1.0287
		1.27	0.24	0.9444	1.5932	1.0343
Shapiro test, W -stat: 0.909			P- value: 0.31		N.D : Yes	
Levene's test, p: 0.005			α: 0.05		HOM : No	

Table 3. Shrinkage in Y-direction

Temp.	Length	Shrinkage	Sorted R.	Percentile	Normal Q	Sample Q
195 °C	15	1.78	-19.74	0.0556	-1.5932	-1.2200
		1.46	-18.65	0.1667	-0.9674	-1.1523
		1.32	-10.43	0.2778	-0.5895	-0.6447
200 °C	15	1.04	-6.13	0.3889	-0.2822	-0.3787
		0.88	-2.84	0.5000	0.0000	-0.1753
		1.28	2.24	0.6111	0.2822	0.1383
205 °C	15	0.53	8.19	0.7222	0.5895	0.5064
		0.34	21.48	0.8333	0.9674	1.3276
		0.47	25.87	0.9444	1.5932	1.5987
Shapiro test, W -stat: 0.939			P- value: 0.57		N.D : Yes	
Levene's test, p: 0.379			α: 0.05		HOM : Yes	

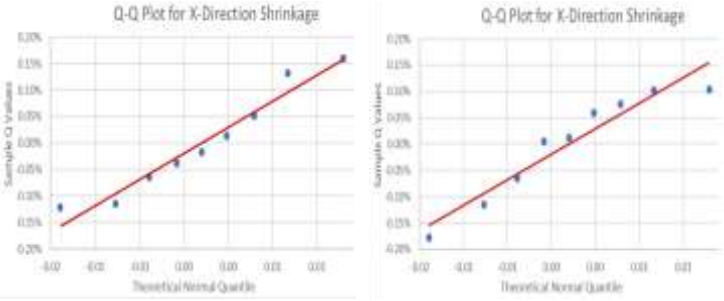

Fig. 1. Quantile-quantile plot diagram for initial specimens

The dimensional data of printed and annealed specimens were confirmed to be normally distributed in both the X-direction (W=0.939, p=0.571) and the Y-direction (W=0.950, p=0.307), based on the Shapiro-Wilk test conducted in Microsoft Excel using the Real Statistics add-in [24]. This outcome was further corroborated by the Q-Q plot in Figure 1, which shows that the data points closely follow the reference line. In addition, Levene's test verified that the assumption of homogeneity of variances was satisfied for shrinkage in both the X-direction, p(0.379), and the Y-direction, p(0.241). Since the assumptions of normality and homoscedasticity were upheld, the use of parametric comparative methods, specifically ANOVA, is statistically justified. The shrinkage data as a function of specimen length at each nozzle temperature are summarized in Table 4, while the results of the ANOVA are presented in Table 5.

Table 4. Shrinkage in X and Y.

Length	195 °C	200 °C	205 °C
	2.98%	2.81%	1.43%
20	2.34%	2.60%	1.55%
	2.92%	2.32%	1.27%
	1.78%	1.04%	0.53%
15	1.46%	0.88%	0.34%
	1.32%	1.28%	0.47%

Table 5. Two-way ANOVA

Variation	*SS*	*df*	*MS*	*F*	*P-value*	*F crit*
Length	0.00069	1	0.000686	132.031	0.00000008	4.7472
Temperature	0.00047	2	0.000234	45.013	0.00000265	3.8853
Interaction	0.00002	2	0.000011	2.151	0.15908312	3.8853
Within	0.00006	12	0.000005			
Total	0.00124	17				

The two-way ANOVA results indicated that both the initial printed length and nozzle temperature were statistically significant determinants of dimensional shrinkage. The length factor exhibited the largest effect ($F=132.03$, $p<0.001$), confirming that shrinkage scales proportionally with specimen length and reflects an intrinsic material response. Nozzle temperature within the 195-205°C range was also highly influential ($F=45.01$, $p=0.001$), underscoring its role as a critical process variable. Elevated nozzle temperatures enhance polymer chain mobility and interlayer diffusion, thereby promoting stress relaxation and increased crystallinity in semi-crystalline polymers such as PLA [24]. This mechanism resembles an in situ annealing effect [25], which strongly governs shrinkage behavior. No significant interaction between temperature and specimen length was observed ($F=2.15$, $p=0.159$), indicating that the influence of thermal conditions on shrinkage operates independently of specimen length. To further delineate temperature effects, post-hoc comparisons were performed using Tukey's HSD test (Table 6), showing that specimens printed at 205°C exhibited significantly lower shrinkage than those printed at 200°C and 195°C ($p < 0.05$), while no significant difference was observed between the 195°C and 200°C groups.

Table 6. Post-hoc (Tukey-Kramer HSD)

Comparation	abs. difference	crit. range	result
195°C to 200°C	0.004537	0.004967	not significant
195°C to 205°C	0.010723	0.004967	significant
200°C to 205°C	0.006187	0.004967	significant

Tukey-Kramer Procedure (df=12, group=3, alpha=0,05, q=3.773)

3.2 Targeted temperature

The results of the initial experiment demonstrated an inverse relationship between nozzle temperature and shrinkage, with higher temperatures leading to reduced dimensional contraction. Based on the preliminary screening results, a subsequent investigation was conducted using specimens fabricated at higher nozzle temperatures of 210°C, 220°C, and 230°C, as illustrated in Fig. 2.

Fig. 2. Targeted specimens

The shrinkage percentages obtained from each experiment are presented in Table 7, while the corresponding group-wise summaries are provided in Table 8.

Table 7. Shrinkage at 210-230°C

Specimen Dimention	Length (mm)	Shrinkage (%)		
		210 °C	220 °C	230 °C
20 x 10 x 10	X=20	1.34	1.04	0.45
		1.24	1.13	0.60
		0.90	1.14	0.70
	Y=10	0.10	0.78	0.20
		0.10	0.87	0.10
		0.59	1.07	0.39
20 x 20 x 20	X=20	0.70	1.10	0.95
		1.00	0.95	0.85
		1.06	1.10	0.65
	Y=20	0.75	1.15	0.75
		0.90	1.29	0.80
		1.10	1.14	0.15
20 x 30 x 30	X=20	1.00	0.80	0.90
		0.75	1.10	1.10
		0.75	1.00	0.94
	Y=30	1.34	0.84	0.67
		1.04	1.37	0.40
		1.41	1.34	0.60

The Shapiro-Wilk test confirmed that the data followed a normal distribution in both the X-direction (W(0.961), p(0.300)) and the Y-direction (W(0.924), p(0.390)). Levene's test indicated that the assumption of homogeneity of variances was satisfied for shrinkage in both the X-direction, p(0.100) and the Y-direction, p(0.059).

Table 8. Descriptive statistics of shrinkage

Length	Temp.	Orien-tation	Count (n)	Shrink-age (%)	Mean	SD
10	210	Y	3	0.10	0.263	0.283
10	220	Y	3	0.78	0.907	0.148
10	230	Y	3	0.20	0.230	0.147
20	210	X	9	1.00	0.971	0.222
20	210	Y	3	0.75	0.917	0.176
20	220	X	9	0.80	1.040	0.110
20	220	Y	3	1.15	1.193	0.053
20	230	X	9	0.90	0.852	0.094
20	230	Y	3	0.75	0.567	0.362
30	210	Y	3	1.34	1.263	0.197
30	220	Y	3	0.84	1.183	0.298
30	230	Y	3	0.67	0.557	0.140

This outcome was further corroborated by the Q-Q plot shown in Fig. 3.

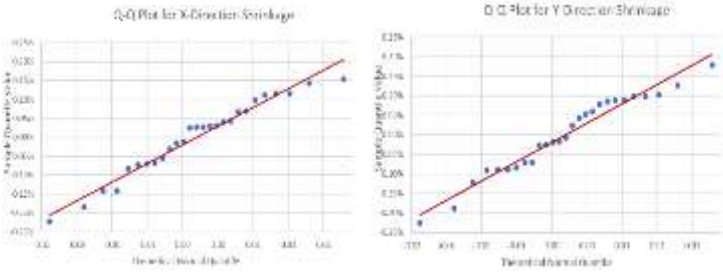

Fig. 3. Quantile-quantile plot diagram for targeted specimens

A three-way ANOVA was conducted to examine the individual and combined effects of specimen length (L), nozzle temperature (T), and measurement direction (D) on shrinkage behavior. The statistical ANOVA outcomes are summarized in Table 9 and graphically illustrated in Fig. 4.

The analysis revealed significant main effects for both specimen length, $F(2,36)=35.27$, $p<0.001$, partial $\eta^2=0.66$, and nozzle temperature, $F(2,36)=30.90$, $p<0.001$, partial $\eta^2=0.63$, indicating large effect sizes and confirming their substantial contributions to shrinkage variability. Measurement direction also exerted a

statistically significant, though comparatively moderate, effect, $F(1,36)=14.98$, $p<0.001$, partial $\eta^2=29$.

Regarding interaction effects, two combinations were significant. The Length×Temperature interaction was substantial, $F(4,36)=7.30$, $p<0.001$, partial $\eta^2=0.45$, while the Temperature×Direction interaction was also statistically significant, $F(2,36)=9.22$, $p<0.001$, partial $\eta^2=0.34$. These findings suggest that the influence of nozzle temperature on shrinkage is conditioned by both specimen length and measurement direction. By contrast, the Length×Direction interaction was non-significant, $F(2,36)=0.00$, $p>0.99$, as was the three-way interaction among Length, Temperature, and Direction, $F(4,36)=0.00$, $p\approx1.00$.

The non-linear trend in mean shrinkage, with the highest values observed at 220°C, indicates that the influence of nozzle temperature on dimensional change during annealing is not monotonic. This behavior is consistent with prior studies showing that nozzle temperature governs melt homogeneity, interlayer diffusion, and residual stress development during FDM processing, which collectively affect dimensional stability after annealing [19], [20]. At intermediate extrusion temperatures, partial stress relaxation may coexist with enhanced molecular mobility and crystallization, resulting in a trade-off between improved interlayer bonding and increased susceptibility to annealing-induced dimensional contraction. Similar non-linear responses and trade-offs between interlayer adhesion and dimensional stability during annealing have been reported for PLA and other semi-crystalline polymers processed by material extrusion [10], [25]. By contrast, higher nozzle temperatures promote more effective interlayer fusion and stress relaxation, thereby reducing dimensional changes during annealing. From a practical perspective, these results highlight the importance of identifying an optimal nozzle temperature window rather than assuming a linear benefit from increasing extrusion temperature.

Table 9. Three-way ANOVA

Variation	*SS*	*df*	*MS*	*F*	*p-value*	*p eta-sq*
Length (L)	1.789639	2	0.8948	35.275	0.000000003	0.6621
Temperature (T)	1.567511	2	0.7838	30.897	0.000000015	0.6319
Direction (D)	0.380017	1	0.3800	14.981	0.000439162	0.2939
L x T	0.741117	4	0.1853	7.304	0.000205308	0.4480
L x D	0.000004	2	0.0000	0.000	0.999921161	0.0000
T x D	0.467778	2	0.2339	9.220	0.000584603	0.3387
L x T x D	0.000006	4	0.0000	0.000	0.999999993	0.0000
Within	0.913212	36	0.0254			
Total	5.859283	53	0.1106			

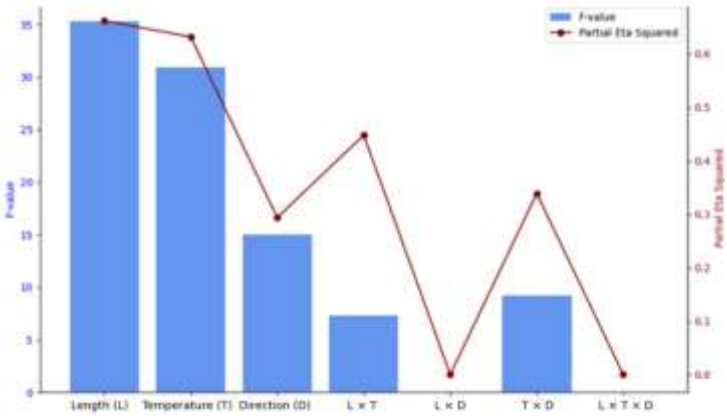

Fig. 4. F-value and p eta-sq (η^2)

Tukey's HSD results presented in Table 10 highlight the relationship between nozzle temperature and shrinkage as a key outcome of this study. The greatest shrinkage was observed at 220°C, which can be attributed to sub-optimal viscoelastic behavior at this processing condition. At this temperature, the polymer melt exhibits sufficiently low viscosity to promote interlayer adhesion; however, the elevated molecular mobility facilitates extensive chain relaxation and crystallization during cooling. This combination enhances volumetric contraction, thereby producing greater shrinkage [26]

Table 10. Tukey's HSD for nozzle temperature

Comparison	Mean Difference (%)	p-value	Significance (α=0.05)
210°C vs. 220°C	-0.00174	0.001	Significant
210°C vs. 230°C	0.0024	< 0.001	Significant
220°C vs. 230°C	0.00414	< 0.001	Significant

The superior performance observed at 230°C can be attributed to more complete polymer melting, which alleviates residual stresses and promotes the formation of a stable amorphous morphology upon cooling. This reduced structural ordering minimizes volumetric contraction, thereby lowering shrinkage [27]. Within the investigated processing window, 230°C is therefore identified as the most effective nozzle temperature.

6 Conclusion

This study shows that dimensional shrinkage in annealed FDM-printed PLA is governed by the combined effects of processing and geometric factors, with nozzle temperature exhibiting the strongest influence among the variables examined. Within the investigated range of 195-230°C, shrinkage displayed a clear dependence on nozzle temperature, with printing at 230°C resulting in the lowest shrinkage and the highest dimensional accuracy ($F(2,36)=30.90$, $p<0.001$). The contribution of its specimen length and measurement direction were smaller, indicating that dimensional stability cannot be attributed to a single controlling parameter. At 220°C, improved interlayer adhesion coincides with enhanced molecular relaxation and crystallization, resulting in greater volumetric contraction during annealing. However, printing at 230°C promotes more complete melting, reducing residual stresses and stabilizing the amorphous phase, thereby suppressing post-annealing shrinkage. Therefore, setting the nozzle temperature to 230°C provides a simple, evidence-based guideline for improving geometric in PLA parts produced under similar processing conditions, while acknowledging potential trade-offs associated with higher thermal exposure. The conclusions are limited to the specific annealing condition and nozzle temperature window examined in this study so that generalization beyond these conditions should be made with caution. Future work should prioritize a more refined control of nozzle temperature in the vicinity of 220-230°C.

References

[1] Cano-Vicent et al., "Fused deposition modelling: Current status, methodology, applications and future prospects," *Additive Manufacturing*, vol. 47, p. 102378, 2021. https://doi.org/10.1016/j.addma.2021.102378

[2] N.-D. Ciobota and G. I. Gheorghe, "3D complex structures through fused deposition modeling as a rapid prototyping technology designed for replacing anatomic parts of the human body," *Bulletin of the Transilvania University of Braşov, Series I: Engineering Sciences*, vol. 16, no. 15, pp. 30–33, 2018. Available: https://www.researchgate.net/publication/330125417

[3] R. C., R. Shanmugam, M. Ramoni, and G. Bk, "A review on additive manufacturing for aerospace application," *Materials Research Express*, 2024. https://doi.org/10.1088/2053-1591/ad21ad

[4] D. Calderone et al., "Optimization of 3D fused deposition modeling printing process for the manufacturing of devices for medical use," pp. 484–489, 2023. https://doi.org/10.1109/metroxraine58569.2023.10405691

[5] L. Chen, N. P. H. Ng, J. Jung, and S. K. Moon, "Additive

manufacturing for automotive industry: Status, challenges and future perspectives," pp. 1431–1436, 2023. https://doi.org/10.1109/ieem58616.2023.10406820
[6] S. F. Iftekar, A. Aabid, A. Amir, and M. Baig, "Advancements and limitations in 3D printing materials and technologies: A critical review," *Polymers*, vol. 15, no. 11, 2023. https://doi.org/10.3390/polym15112519
[7] M. Johar et al., "Dimensional stability of poly(lactic acid) (PLA) parts fabricated using fused deposition modelling (FDM)," *Progress in Rubber, Plastics and Recycling Technology*, 2024. https://doi.org/10.1177/14777606241262882
[8] M. S. Alsoufi et al., "Experimental characterization of the influence of nozzle temperature in FDM 3D-printed pure PLA and advanced PLA," *American Journal of Mechanical Engineering*, vol. 7, no. 2, pp. 45–60, 2019. https://doi.org/10.12691/AJME-7-2-1
[9] S. Li, K. Wang, J. P. M. Correia, Y. Li, and S. Ahzi, "Investigating gradient temperature control for enhanced interfacial bonding behavior in material extrusion 3D printing continuous fiber-reinforced polymer composites," *European Journal of Mechanics A/Solids*, p. 105349, 2024. https://doi.org/10.1016/j.euromechsol.2024.105349
[10] T. Joseph et al., "3D printing of polylactic acid: Recent advances and opportunities," *The International* Journal *of Advanced Manufacturing Technology*, vol. 125, nos. 3–4, pp. 1015–1035, 2023. https://doi.org/10.1007/s00170-022-10795-y
[11] Z. Liu et al., "A critical review of fused deposition modeling 3D printing technology in manufacturing polylactic acid parts," *The International Journal of Advanced* Manufacturing *Technology*, vol. 102, no. 9, pp. 2877–2889, 2019. https://doi.org/10.1007/s00170-019-03332-x
[12] Y. Li et al., "Blending and functionalisation modification of 3D-printed polylactic acid for fused deposition modeling," *Reviews on Advanced Materials Science*, vol. 62, no. 1, p. 20230140, 2023. https://doi.org/10.1515/rams-2023-0140
[13] C. Benwood et al., "Improving the impact strength and heat resistance of 3D-printed models: Structure, property, and processing correlations during fused deposition modeling of poly(lactic acid)," *ACS Omega*, vol. 3, no. 4, pp. 4400–4411, 2018. https://doi.org/10.1021/acsomega.8b00129
[14] E. H. Tümer and H. Y. Erbil, "Extrusion-based 3D printing applications of PLA composites: A review," *Coatings*, vol. 11, no. 4, 2021. https://doi.org/10.3390/coatings11040390
[15] A. Natayu et al., "Effect of annealing on the mechanical properties of fused deposition modeling 3D-printed PLA," *Rekayasa Mesin*, vol. 15, no. 3, pp. 1343–1351, 2024. https://doi.org/10.21776/jrm.v15i3.1625
[16] M. Evan, T. J. Suteja, and S. Tjandra, "The influence of annealing temperature and holding time near glass transition temperature on the tensile strength of fused deposition modeling-printed polylactic acid," *Jurnal Polimesin*, vol. 21, no. 1, pp. 25–28, 2023. Available: https://repository.ubaya.ac.id/43524/
[17] N. Zohdi and R. C. Yang, "Material anisotropy in additively manufactured polymers and polymer composites: A review," *Polymers*, vol. 13, no. 19, 2021. https://doi.org/10.3390/polym13193368
[18] J. Butt and R. Bhaskar, "Investigating the effects of annealing on the mechanical properties of FFF-printed thermoplastics," *Journal of Manufacturing and Materials Processing*, vol. 4, no. 2, 2020. https://doi.org/10.3390/jmmp4020038
[19] F. Rivera-López et al., "Effects of nozzle temperature on mechanical properties of polylactic acid specimens fabricated by fused deposition modeling," *Polymers*, vol. 16, no. 13, p. 1867, 2024. https://doi.org/10.3390/polym16131867
[20] S. Liparoti et al., "Fused filament deposition of PLA: The role of interlayer adhesion in the mechanical performances," *Polymers*, vol. 13, no. 3, 2021. https://doi.org/10.3390/polym13030399
[21] X. Wei et al., "Geometric accuracy and dimensional precision in 3D printing-based gear manufacturing: A study on interchangeability and forming precision," Polymers, vol. 17, no. 3, 2025. https://doi.org/10.3390/polym17030416
[22] L. Lin and C. Xu, "Arcsine-based transformations for meta-analysis of proportions: Pros, cons, and alternatives," *Health Science Reports*, vol. 3, no. 3, e178, 2020. https://doi.org/10.1002/hsr2.178
[23] L. Laurencelle and D. Cousineau, "Analysis of proportions using arcsine transform with any experimental design," *Frontiers in Psychology*, vol. 13, 2023. https://doi.org/10.3389/fpsyg.2022.1045436
[24] K. Elhattab, S. B. Bhaduri, and P. Sikder, "Influence of fused deposition modelling nozzle temperature on the rheology and mechanical properties of 3D-printed tricalcium phosphate/polylactic acid composites," *Polymers*, vol. 14, no. 6, p. 1222, 2022. https://doi.org/10.3390/polym14061222
[25] B. Dillon et al., "Influence of annealing and biaxial expansion on the properties of poly(L-lactic acid) medical tubing," *Polymers*, vol. 11, no. 7, 2019. https://doi.org/10.3390/polym11071172
[26] D. P. Simunec et al., "Facilitating the additive manufacture of high-performance polymers through polymer blending: A review," *European Polymer Journal*, vol. 201, p. 112553, 2023. https://doi.org/10.1016/j.eurpolymj.2023.112553
[27] M. F. Afrose et al., "Effects of part build orientation on fatigue behaviour of FDM-processed PLA material," *Progress in Additive Manufacturing*, vol. 1, no. 1, pp. 21–28, 2016. https://doi.org/10.1007/s40964-015-0002-3